MOLECULAR AND CELLULAR BIOLOGY, Sept. 2006, p. 6957–6970 Vol. 26, No. 18
0270-7306/06/$08.00+0 doi:10.1128/MCB.00075-06

Rac1 Is Crucial for Hair Follicle Integrity but Is Not Essential for Maintenance of the Epidermis†

Anna Chrostek,[1]§ Xunwei Wu,[1]‡ Fabio Quondamatteo,[2] Rong Hu,[1] Anna Sanecka,[1] Catherin Niemann,[3] Lutz Langbein,[4] Ingo Haase,[5] and Cord Brakebusch[1]*

Heisenberg Group "Regulation of Cytoskeletal Organization," Max Planck Institute of Biochemistry, Martinsried, Germany[1]; Department of Histology, Georg August University of Göttingen, Göttingen, Germany[2]; Institute of Pathology, Center for Molecular Medicine (CMMC), University of Cologne, Cologne, Germany[3]; Department of Cell Biology, German Cancer Research Center, Heidelberg, Germany[4]; and Department of Dermatology, Center for Molecular Medicine (CMMC), University of Cologne, Cologne, Germany[5]

Received 12 January 2006/Returned for modification 4 February 2006/Accepted 3 July 2006

Rac1 is a small GTPase that regulates the actin cytoskeleton but also other cellular processes. To investigate the function of Rac1 in skin, we generated mice with a keratinocyte-restricted deletion of the *rac1* gene. Rac1-deficient mice lost nearly all of their hair within a few weeks after birth. The nonpermanent part of mutant hair follicles developed constrictions; lost expression of hair follicle-specific keratins, E-cadherin, and α6 integrin; and was eventually removed by macrophages. The permanent part of hair follicles and the sebaceous glands were maintained, but no regrowth of full-length hair follicles was observed. In the skin of mutant mice, epidermal keratinocytes showed normal differentiation, proliferation, cell-cell contacts, and basement membrane deposition, demonstrating no obvious defects of Rac1-deficient epidermis in vivo. In vitro, Rac1-null keratinocytes displayed a strong spreading defect and slightly impaired adhesion. These data show that Rac1 plays an important role in sustaining the integrity of the lower part of hair follicles but not in maintenance of the epidermis.

Rac1 is a ubiquitously expressed member of the Rho family of small GTPases (8, 21). Like other GTPases, it cycles between an inactive GDP-bound form and an active GTP-bound form. Guanine nucleotide exchange factors catalyze Rac1 activation, while GTPase-activating proteins promote the hydrolysis of GTP to GDP, resulting in the inactivation of Rac1. Different pathways involving integrins, growth factor receptors, or cadherin signaling can induce Rac1 activation (8). Furthermore, Rac1 activity can be regulated by cross talk with other Rho GTPases. Only in its active form can Rac1 associate with different effector molecules such as PAKs, WAVE, and IQGAP to initiate cellular responses, for example, formation of lamellipodia or Jun N-terminal protein kinase (JNK) activation. The focus of our interest is the in vivo function of Rac1 in skin.

The skin can be roughly divided into the epidermis, consisting mainly of keratinocytes, and the dermis; these two components of skin are separated by the basement membrane (BM). The proliferating basal keratinocytes, which express keratin 5 (K5) and keratin 14 (K14), adhere to the BM. Basal keratinocytes mature into suprabasal keratinocytes. This transition is characterized by loss of contact with the BM, a halt in proliferation, and downregulation of K5 and K14 accompanied by upregulation of K1 and K10. Finally, suprabasal keratinocytes undergo an apoptosis-related process called terminal differentiation which results in the formation of a layer of dead cornified cells, the stratum corneum. This layer is a main component of the skin barrier and protects the animal against physical, chemical, and biological stress. Hair follicles (HFs) are formed during embryogenesis as outgrowths of the epidermis. Continuous with the basal keratinocyte layer is the outer root sheath (ORS) of the HF. Cross talk between fibroblasts of the dermal papilla and keratinocytes in the hair bulb region induces proliferation and later differentiation of transient amplifying stem cells into different keratinocyte lineages of HFs, i.e., the companion layer (CL) directly adjacent to the ORS, the inner root sheath (IRS) with its various compartments (Henle layer, Huxley layer, IRS cuticle), and the hair shaft (HS) with the hair cuticle, cortex, and (if it exists) medulla (10, 18). After HF morphogenesis, HFs undergo cyclic phases of involution (catagen), during which the lower part of the HF is lost, a dormant period (telogen), and a growth phase (anagen), when cross talk between dermal papilla cells and progenitor cells in the hair bulge region leads to the restoration of a complete HF with an ORS, a CL, an IRS, an HS, and a hair bulb.

Conflicting results have been reported regarding the Rac1-dependent regulation of cell-cell contacts between keratinocytes. In primary human keratinocytes, dominant negative Rac1 and constitutively active Rac1 were shown to lead to the disruption of cadherin-dependent cell-cell adhesion between keratinocytes (3, 4). However, in mouse keratinocytes deficient in the Rac1-activating guanine nucleotide exchange factor Tiam-1, impaired cell-cell contacts could be rescued by over-

* Corresponding author. Present address: Group of Developmental Biology, Institute of Molecular Pathology, Copenhagen University, 2100 Copenhagen, Denmark. Phone: 0045-353-26043. Fax: 0045-353-26081. E-mail: cord@pai.ku.dk.

† Supplemental material for this article may be found at http://mcb.asm.org/.

‡ Present address: Group of Developmental Biology, Institute of Molecular Pathology, Copenhagen University, 2100 Copenhagen, Denmark.

§ Present address: Department of Molecular Medicine, Max Planck Institute of Biochemistry, Martinsreid, Germany.

expression of constitutively active Rac1 (12). Taken together, the data indicate a complex relationship between Rac1 activity and maintenance of cell-cell contacts between keratinocytes.

Recently, it was shown that induced loss of Rac1 in keratinocytes of adult mice leads to depletion of epidermal stem cells (1). In the skin of these mice, an increased proliferation of basal keratinocytes, corresponding to an enhanced expression of c-Myc, was observed a few days after induction of the knockout (KO). Within 11 to 15 days, α6β4 integrin expression and hemidesmosomes were lost, HF organization was impaired, and a partial or complete loss of epidermis occurred. In vitro, knockdown of Rac1 in cultured human keratinocytes resulted in reduced clonal growth and increased terminal differentiation. It was concluded that Rac1 plays a critical role in controlling exit from the stem cell niche, which leads to loss of epidermal stem cells in vivo after deletion of the *rac1* gene.

We generated mice with a keratinocyte-restricted deletion of the *rac1* gene independently and analyzed skin and HF development and maintenance. We observed severe hair loss due to restricted removal of the lower part of the HFs but, surprisingly, no major defect in the maintenance of the epidermis.

MATERIALS AND METHODS

Generation of Rac1 mutant mice. A fragment of the *rac1* gene including exon 3 was used as a probe for screening the 129/Sv mouse genomic PAC library RPCI21 (Geneservice Ltd.) (14). The targeting vector contained a fragment of the *rac1* gene (including exons 2 and 3) with a *neo-tk* selection cassette (flanked by *loxP* sites) introduced downstream of exon 3 and an additional *loxP* site upstream of exon 3 (Fig. 1A). The construct was electroporated into R1 embryonic stem (ES) cells (129/Sv), and homologous recombinants were identified by Southern blot analysis of HindIII-digested DNA with an external probe (Fig. 1B). The selection cassette was removed from ES cells by transient transfection with Cre recombinase (pIC-Cre plasmid; kind gift from Werner Müller, University of Cologne, Cologne, Germany), and cells were selected for lack of the cassette with FIAU (2′-fluoro-2′-deoxy-1-β-D-arabinofuranosyl-5-iodouracil)-supplemented growth medium (0.2 μM FIAU). Clones with a floxed exon 3 were identified with an internal probe after BamHI digestion (Fig. 1B′) and used for the generation of germ line chimeras by blastocyst injection. Male chimeras were crossed with C57BL/6 mice. Offspring carrying the conditional allele were identified by Rac1 PCR genotyping with primers distinguishing between the wild-type and floxed alleles (5′-GTCTTGAGTTACATCTCTGG-3′, 5′-CTGACGCCAA CAACTATGC-3′) (Fig. 1A, green arrows). Heterozygotes were mated to obtain homozygote animals, which were subsequently intercrossed with mice expressing Cre recombinase under the control of the K5 promoter (16). The presence of the null allele in mice carrying both the Rac1 conditional allele and the Cre-encoding transgene was confirmed by KO PCR (5′TTGATTTCCATAAAGCTTATAAC-3′, 5′-ACCAAGTGCCCAATCGGC-3′) (Fig. 1A, red arrows). Animals used for experiments were genotyped by Rac1 and Cre PCR (Fig. 1C). The mice were kept in a barrier facility according to the German rules of animal welfare.

Effects of 4-hydroxy-tamoxifen (4OHT) on epidermis were analyzed in control and Rac1-deficient adult mice (2 to 3 months old). Every third day for 15 days, 250 μl of acetone or 250 μl of a 4OHT-acetone solution (10 mg/ml; Sigma) was applied to a clipped area of back skin. Fragments of the treated skin were isolated 1 day or 2 weeks after the last application, and hematoxylin-eosin (HE) staining of paraffin-embedded sections was performed.

Histology, immunohistochemistry, and electron microscopy (EM). Fragments of murine back skin where either directly frozen in Shandon Cryomatrix compound (Thermo Electron Corporation) or fixed overnight in fresh 4% paraformaldehyde (PFA) in phosphate-buffered saline (PBS) (pH 7.4) and embedded in paraffin. HE staining of 6-μm-thick paraffin sections was performed according to standard protocols. Immunofluorescence (IF) staining of 10-μm-thick cryosections (fixed for 20 min in 4% PFA in PBS, permeabilized for 5 min on ice in 0.1% Triton X-100 in PBS, and blocked with 3% bovine serum albumin [BSA] in PBS) was performed with the following antibodies diluted to a concentration recommended by the manufacturer in 1% BSA in PBS: K14, K10, K6, loricrin (all from Covance), K6irs2, K6irs4, Hb2, vimentin (all kindly provided by Lutz Langbein) (9), E-cadherin (Zymed), β-catenin, α-catenin (both from Sigma), desmoplakin (Research Diagnostics), laminin 5 (laminin γ2 LE4-6; LN5), nidogen-1 (both kindly provided by Takako Sasaki, Martinsried, Germany), β4 integrin (346-11A), α6 integrin-FITC (fluorescein isothiocyanate) (GoH3), Mac1-biotin (Ha2/5; all from BD Pharmingen), Cy3-conjugated streptavidin, and Cy3-conjugated secondary antibodies (all from Jackson ImmunoResearch). Nuclear DNA was visualized with 4′,6′-diamidino-2-phenylindole (DAPI; Sigma). Pictures were taken with a confocal microscope (Leica).

The presence of apoptotic cells in the skin was evaluated with a TUNEL (terminal deoxynucleotidyltransferase-mediated dUTP-biotin nick end labeling) assay. Staining of cryosections was performed according to the manufacturer's instructions (In Situ Cell Death Detection Kit; Roche). Proliferation of keratinocytes in the epidermis was analyzed with paraffin sections from mice sacrificed 2 h after intraperitoneal injection of a bromodeoxyuridine (BrdU) solution (50 μg/g of body weight). Proliferating cells were visualized with a peroxidase-conjugated anti-BrdU antibody (Roche). More than 4,000 cells were counted in each control and mutant epidermis sample.

Skin samples for EM were prepared as described previously (5). For a more-detailed analysis of desmosomes and adherent junctions, additional samples were prepared by the following protocol. Samples of back skin were isolated and quickly dissected, while immersed in 0.1 M Na-cacodylate buffer supplemented with 2 mM $CaCl_2$, into small fragments of about 1 mm^3. Subsequently, samples were fixed for at least 24 h in a mixture of 2% glutaraldehyde and 4% PFA in 0.1 mM Na-cacodylate plus 2 mM $CaCl_2$ buffer. After being washed, skin was postfixed in 1% OsO_4 (osmium tetroxide) in 0.1 mM Na-cacodylate plus 2 mM $CaCl_2$ buffer, dehydrated in a graded ethanol series, and embedded in Epon. For orientation purposes, semithin sections (1 μm) were cut and stained with Richardson's solution. Ultrathin sections (90 nm) were cut with a Reichert-Jung ultramicrotome, collected on Formvar-coated nickel grids, and stained with uranyl acetate for 10 min and with lead citrate for 7 min. Samples were examined with a LEO 906E electron microscope (Zeiss).

Epidermal lysates, Western blot analysis, and GTPase activity assay. Epidermis of 3-day-old mice was isolated with dispase II as previously described (6). Isolation of epidermis keratinocytes from older mice was carried out according to a modified protocol of Romero and colleagues (17). Sacrificed mice were shaved and sequentially washed in an iodine solution, distilled water, and 70% ethanol. After peeling off and removing the subcutaneous layer, the skin was cut into fragments, washed for 5 min in PBS containing antibiotics, and incubated for 50 min at 37°C in 0.8% trypsin (Invitrogen) in PBS. Separated epidermis was shaken for 5 min at 37°C in low-calcium MEM (minimal essential medium) containing 0.25 mg/ml DNase I (both Sigma) and 8% fetal calf serum (FCS; Gibco) treated with Chelex (Bio-Rad). The suspension was filtered through a 70-μm cell strainer (BD Biosciences), and collected keratinocytes were washed once with cold PBS. Subsequently, cells were lysed in ice-cold lysis buffer (150 mM NaCl, 1% Triton X-100, 1 mM EDTA, 1 mM NaF, 1 mM Na_3VO_4, 50 mM Tris, pH 7.6) containing protease inhibitor cocktail tablets (Complete Mini, EDTA free; Roche). Separation by sodium dodecyl sulfate-polyacrylamide gel electrophoresis and Western blotting were carried out according to standard protocols.

For GTPase activity assay, freshly isolated cells were lysed in 750 μl NP-40 lysis buffer (100 mM NaCl, 1% Nonidet P-40 [Sigma], 10% glycerol, 2 mM $MgCl_2$, 1 mM NaF, 1 mM Na_3VO_4, 50 mM Tris-HCl, pH 7.4) supplemented with protease inhibitor cocktail tablets (Complete Mini, EDTA free; Roche) and containing biotinylated PAK-CRIB peptide (Cdc42/Rac interactive binding motif in PAK1B; provided by J. Collard) (15). Lysates were clarified by centrifugation at 20,000 × *g* for 10 min at 4°C and then incubated with glutathione *S*-transferase–rhotekin (fusion protein of the Rho-binding domain of the Rho effector protein) coupled to glutathione-conjugated Sepharose beads (Sigma) for 45 min at 4°C. The lysate was subsequently incubated with streptavidin-conjugated agarose beads for 30 min at 4°C to sequester Cdc42-PAK-CRIB. Beads with bound RhoA and Cdc42 where washed three times with lysis buffer and resuspended in 2× sodium dodecyl sulfate-polyacrylamide gel electrophoresis sample buffer. Proteins were detected by Western blotting.

The following primary antibodies were incubated with membranes under the conditions and at the concentrations suggested by the manufacturers: Rac1 (clone 102), Cdc42 (clone 44; both from Transduction Laboratories), Rac1 (clone 23A8; Upstate), Rac3 (kind gift from Ivan de Curtis, San Rafaele Scientific Institute, Milan, Italy) (2), RhoA (119), c-Myc (N-262), IκB-α (C-21), Rac2 (all from Santa Cruz), phospo-Akt (Ser473), Akt, phospo-p38, p38 mitogen-activated protein kinase (all from Cell Signaling), phospho-JNK (Biosource, Cell Signaling), JNK (Biosource), tubulin (YL1/2; kindly provided by Jürgen Wehland, GBF, Braunschweig, Germany), and glyceraldehyde-3-phosphate dehydrogenase (GAPDH; Chemicon). Anti-rat immunoglobulin G (IgG; Jackson ImmunoResearch), anti-mouse IgG (Bio-Rad), and ant-rabbit IgG (Bio-Rad, Daco)

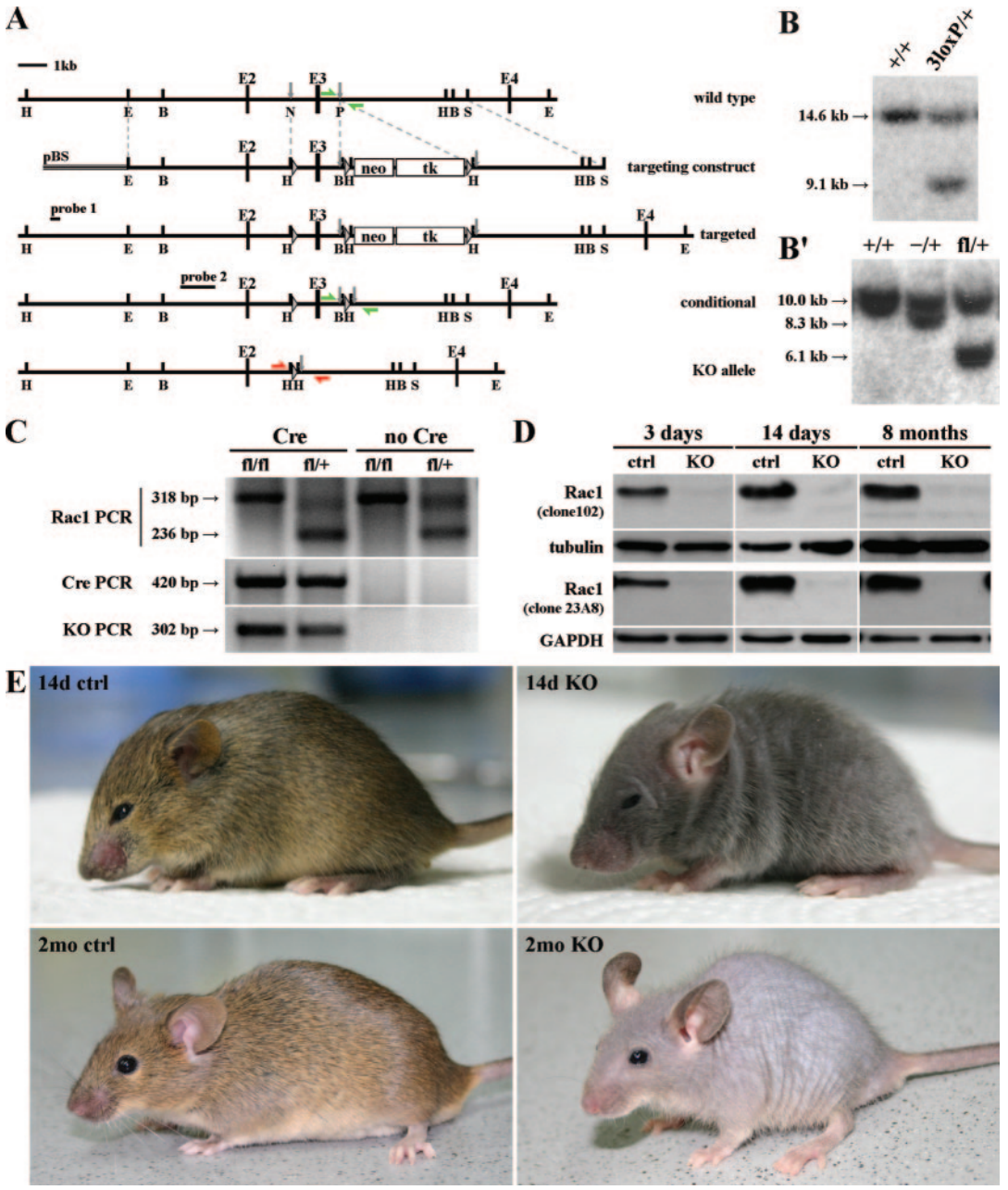

FIG. 1. Generation of mice with a keratinocyte-restricted deletion of the *rac1* gene. (A) Scheme of the targeting strategy. Homologous recombination of the targeting construct into the *rac1* gene of ES cells introduced a *loxP* site (triangle) upstream of exon 3 (E3) and a floxed *neo-tk* selection cassette (white boxes) downstream of it (targeted). Removal of the selection cassette by transient Cre transfection resulted in a floxed exon 3 (conditional). Cre-mediated recombination led to the deletion of exon 3 (KO allele). H, HindIII; E, EcoRI; B, BamHI; S, SalI; N, NotI; P, SpeI; pBS, BlueScript plasmid; probe 1 and probe 2, external and internal probes for Southern blot analysis, respectively; green arrows, Rac1 PCR primers; red arrows, KO PCR primers. (B) Southern blot analysis of targeted ES cells. Genomic DNA was cut with HindIII and hybridized with the external probe (probe 1). 14.6 kb, wild type (+); 9.1 kb, targeted allele (3loxP). (B′) Southern blot analysis of ES cells transiently transfected with Cre recombinase. Genomic DNA was cut with BamHI and hybridized with the internal probe (probe 2). 10.0 kb, wild type (+); 8.3 kb, KO (−); 6.1 kb, conditional allele (fl). (C) Genotyping of mice by genomic PCR performed on tail DNA. Rac1 PCR gave rise to two products, 318 bp for the conditional allele (fl) and 236 bp for the wild-type allele (+). Cre PCR resulted in a 420-bp product when the *cre* transgene was present (Cre). KO PCR gave rise to a 302-bp product when the KO allele was present. (D) Western blot assay for Rac1 content in epidermal lysates from 3-day-, 14-day-, and 8-month-old mice. Analysis was performed with two different antibodies. Mutant mice had already lost the Rac1 protein at 3 days of age. There was no increase in Rac1 protein levels in the epidermis of older mutant mice. (E) Pictures of 14-day-old and 2-month-old control (ctrl) and mutant (KO) mice. Rac1-deficient mice lost nearly all of their hair within a few weeks but did not develop blisters or wounds.

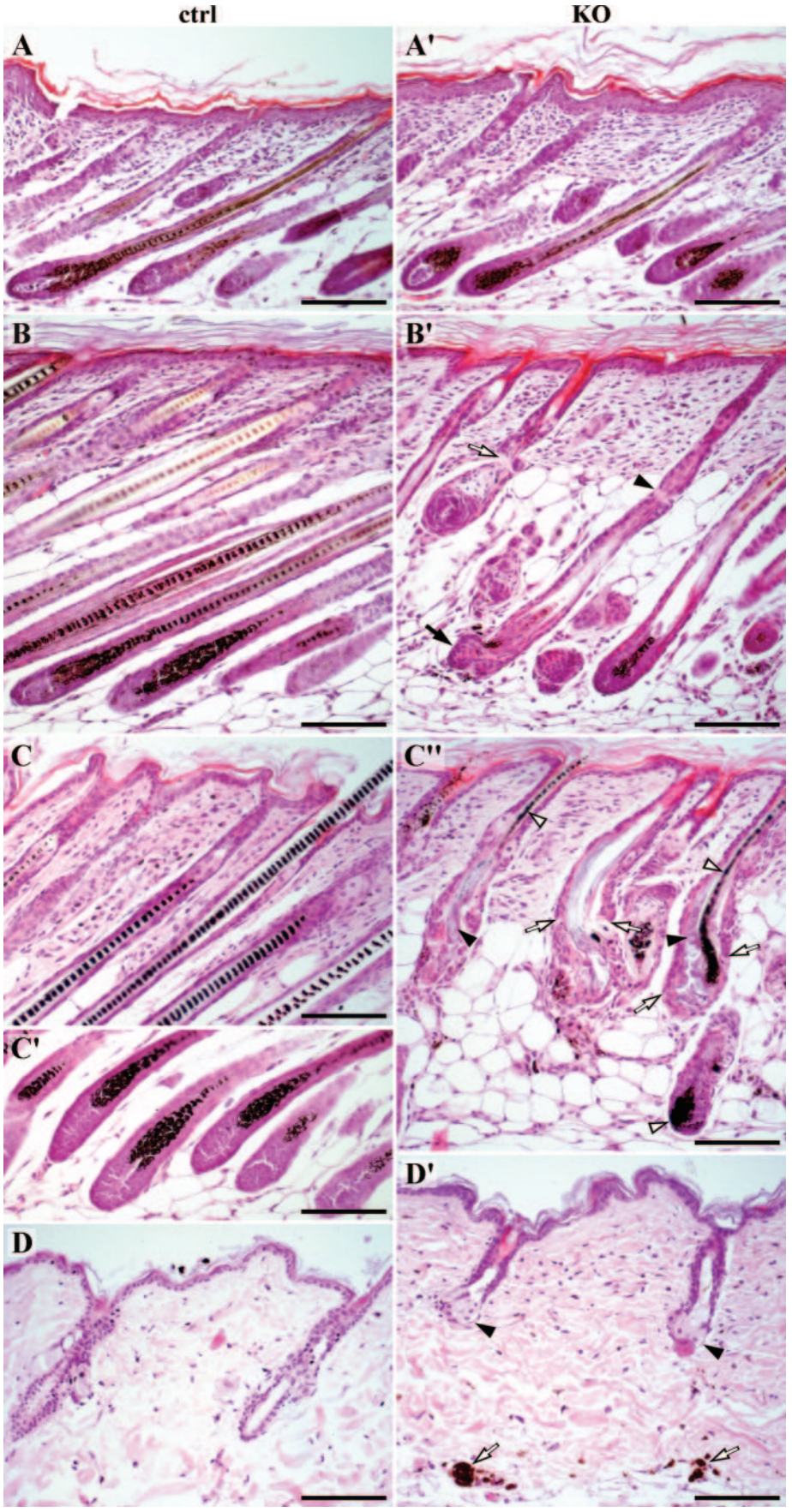
ctrl
KO
A
A'
B
B'
C
C''
C'
D
D'

horseradish peroxidase-conjugated secondary antibodies were used and subsequently visualized with Western Lightning Chemiluminescence Reagent (Perkin-Elmer). The signal was captured on Hyperfilm (Amersham Biosciences).

RNA isolation and quantitative real-time PCR. Total RNA was extracted from freshly isolated keratinocytes (obtained as described above) with TRIzol reagent (Invitrogen) according to the manufacturer's protocol. First-strand synthesis of cDNA was performed on 1 μg of total RNA with SuperScript III reverse transcriptase (Invitrogen) and random primers in a 20-μl reaction volume. Real-time PCR was performed with two sets of RhoG-specific primers (set 1, 5′-TGAGA GCCCAGCCTGATAC-3′ and 5′-ATCGGTGTTGGGTTAAGCAC; set 2, 5′-CTGTTTCTCCATTGCCAGTC-3′ and 5′-GGCTCTCAGGTCCTTC-3′) and GAPDH primers (reference gene) and iQ SYBR Green Supermix (Bio-Rad). Triplicate repeats were prepared for each sample, and the amplification progress was monitored in an iCycler (Bio-Rad). Results were evaluated with software provided with the thermocycler.

Primary keratinocyte in vitro culture. Primary keratinocytes for in vitro experiments were isolated from adult mice (3 to 8 months old) as described above, but the DNase I incubation step was longer (30 min) and washing after filtration was done with DNase I medium instead of PBS. Cells were resuspended and cultured at 34°C and 5% CO_2 in low-calcium MEM (Sigma) supplemented with 5 μg/ml insulin, 10 ng/ml epidermal growth factor, 10 μg/ml transferrin, 10 μM phosphoethanolamine, 10 μM ethanolamine (all from Sigma), 0.36 μg/ml hydrocortisone (Calbiochem), 2 mM L-glutamine (Gibco), 100 U/ml penicillin, 100 μg/ml streptomycin (both from PAA Laboratories), and 8% FCS (Gibco) treated with Chelex (Bio-Rad).

Keratinocytes were seeded on plastic tissue culture dishes (Falcon) coated with collagen I and fibronectin (Col/FN) or with LN5-rich (LN) matrix at a density of 6×10^6 cells per dish (10-cm diameter). The Col/FN surface was prepared by incubating dishes for 2 h at 37°C with a coating medium containing 30 μg/ml Vitrogen (bovine collagen type I; Cohesion), 10 μg/ml fibronectin (Invitrogen), 100 μg/ml BSA (PAA Laboratories), 20 mM HEPES (pH 7.3; Sigma), and 1 mM $CaCl_2$ in MEM (Sigma). The LN matrix was deposited by RAC-11P/SD squamous cell carcinoma cells (20). In short, cells were grown to confluence in high-glucose Dulbecco's MEM with 10% FCS (both from Gibco) and then removed by overnight treatment with 20 mM EDTA in PBS (at 4°C) as previously described (7).

Adhesion assay, live-cell imaging, and spreading analysis. For adhesion assay, 96-well plates were coated with Col/FN (30 μg/ml Vitrogen, 10 μg/ml fibronectin in PBS, overnight at 4°C) or with LN matrix prepared as described above. Plates were washed with PBS and blocked with 1% BSA (PAA Laboratories) in PBS for 90 min at 37°C. Freshly isolated keratinocytes (from 8-month-old mice), resuspended in normal growth medium without FCS, were seeded in the plates and incubated for 1 to 2 h at 37°C. Nonattached cells were removed by washing with PBS, and cell adhesion was estimated in a colorimetric assay based on a *p*-nitrophenyl *N*-acetyl-β-D-glucosaminide (Sigma) reaction. Absorbance was measured at 405 nm with a plate reader (Dynatech MR5000).

Live-cell recordings of freshly isolated keratinocytes (from 8-month-old mice) were started immediately after seeding on Col/FN-coated plastic and conducted for 42 h (at 37°C, 5% CO_2), with a Zeiss Axiovert microscope. Images were captured every 20 min with a motor-controlled charge-coupled device camera (Hamamatsu OrcaER). Evaluation and processing of images were performed with the Metamorph software (Universal Imaging Corporation). Cell size for spreading analysis was assessed by measuring the pixel area of 30 to 40 randomly picked cells on pictures taken at indicated time points.

Immunohistochemistry and fluorescence-activated cell sorter (FACS) analysis of primary keratinocytes. For IF staining, primary keratinocytes were seeded on glass chamber slides (Nunc) coated with Col/FN (coating medium) or LN matrix (prepared as described above). At chosen time points, cells were briefly rinsed in PBS, fixed for 10 min in cold 4% PFA, permeabilized for 15 min with 0.1% Triton X-100, and blocked in 2% BSA (all in PBS). F-actin was detected by using FITC-conjugated phalloidin (Molecular Probes) and focal contacts with anti-paxillin antibody (Transduction Laboratories). Apoptotic cells were visualized with anti-caspase 3 cleaved (Asp175) antibody (Cell Signaling), and terminally differentiated cells were visualized with anti-loricrin antibody (Covance); 800 to 900 cells were counted in each case. Primary antibodies were detected with Cy3-conjugated anti-mouse or anti-rabbit IgG antibodies (Jackson ImmunoResearch), and nuclei were detected with DAPI (Sigma). All antibodies were diluted in 1% BSA in PBS.

Integrin expression on the cell surface was assessed by FACS analysis. After isolation, keratinocytes were labeled with the following antibodies: α1 (Ha31/8) detected with FITC-conjugated anti-hamster IgG cocktail (G70-204, G94-56), α2-FITC (Ha1/29), α4-phycoerythrin (9C10), α5-biotin (5H10-27), α6-FITC (GoH3), αv-biotin (RMV-7), β1-FITC (Ha2/5), β2-biotin (C71.16), β3-biotin (2C9.G2), β7-biotin (2C3.G2), and β4 (346-11A) detected with FITC-conjugated anti-rat IgG2a (RG7/1.30; all from BD Pharmingen). Biotinylated antibodies were detected with Cy5-streptavidin (Jackson ImmunoResearch). The measurements were conducted with the FACScalibur flow cytometry system (BD).

RESULTS

Generation of mice with a keratinocyte-restricted deletion of the *rac1* gene. With the *cre-loxP* system, we generated Rac1 conditional KO mice (Fig. 1A, B, and B′; see Materials and Methods). In order to reduce the risk of perturbing regulatory elements of the promoter of the *rac1* gene or possible upstream genes, we decided to flank exon 3, rather than exon 1, with *loxP* sites. Exon 3 encodes amino acids 37 to 75, which form a part of the core effector domain and the complete switch II region, both of which are essential for Rac1 function. Theoretical splicing from exon 2 to exon 4 or to another downstream exon would result in a frameshift and premature termination of Rac1 translation. Only unrelated amino acids would be added after the first 36 amino acids encoded by exons 1 and 2. Therefore, any potential truncated protein could not be functional.

Mutant mice carrying two modified alleles of the *rac1* gene and a Cre-encoding transgene under the control of the K5 promoter (Rac1 [fl/fl] and Cre; Fig. 1C) showed almost complete loss of Rac1 in epidermal lysates isolated from 3-day-, 14-day-, and 8-month-old mice. The absence of the protein was shown by Western blotting with two different monoclonal antibodies (clones 102 and 23A8; Fig. 1D). Control littermates heterozygous for the conditional gene for Rac1 and expressing the Cre recombinase (Rac1 [fl/+] and Cre; Fig. 1C) had normal amounts of Rac1 protein.

Rac1-deficient mice were born close to the Mendelian ratio and were indistinguishable from control animals at birth. However, within the first week after birth it became obvious that mutant mice grew less hair and displayed progressive hair loss. At 2 months of age, nearly all hair was lost (Fig. 1E). No regrowth of hair was detected up to 24 months of age (data not shown). Interestingly, a few evenly spaced, frail hairs remained in Rac1-deficient mice, suggesting that a small subpopulation of HFs either does not cycle or can cycle independently of

FIG. 2. Aberrant HF morphogenesis in the absence of Rac1. HE staining of back skin sections from 3-day-old (A-A′), 9-day-old (B-B′), 14-day-old (C-C″), and 13-month-old (D-D′) control (ctrl) and mutant (KO) mice was conducted to analyze HF morphogenesis. (A′) Three-day-old mutant HFs still looked normal. (B′) HFs of 9-day-old mutant mice showed constrictions (arrowhead), kinks (white arrow), and distorted hair bulbs (black arrow). (C″) At 14 days, nearly all mutant HFs had severe defects. Widening of the lower regions, distortions in the pattern and shape of HSs (white arrowheads), disruptions of the ORS (white arrows), and abnormal cells inside the HFs (black arrowheads) were observed. (D″) In 13-month-old Rac1-deficient skin, the lower parts of the HFs were completely missing, while SGs became enlarged (arrowheads). Infundibula looked normal. Deposits of HS melanin were found in the subcutaneous layer of mutant skin (arrows). Bars, 100 μm.

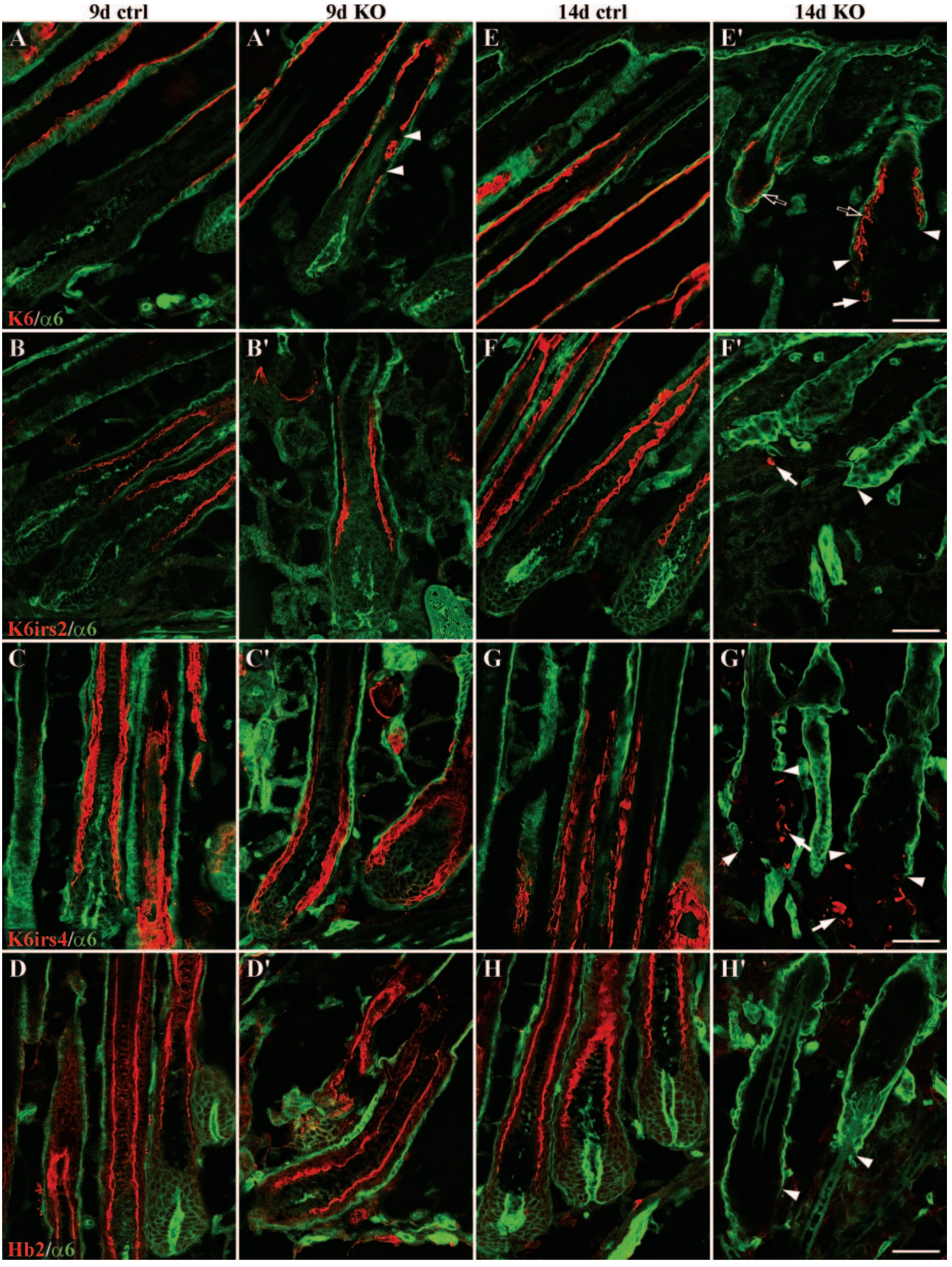
9d ctrl
9d KO
14d ctrl
14d KO
A
A'
E
E'
K6/α6
B
B'
F
F'
K6irs2/α6
C
C'
G
G'
K6irs4/α6
D
D'
H
H'
Hb2/α6

Rac1 (Fig. 1E, 2mo KO). Mutant mice had a slightly reduced body weight but were fertile and showed no increased death rate.

Defective HF morphogenesis in the absence of Rac1. To investigate the hair loss in Rac1-deficient mice, we performed HE staining of back skin sections at different time points. While HFs of 3-day-old mutant mice still looked normal (Fig. 2A and A′), 9-day-old mutant mice already had many aberrant HFs (Fig. 2B and B′) displaying constrictions (black arrowhead), a kinked follicle shape (white arrow), or diffuse thickening of the hair bulb region (black arrow). At 14 days, the phenotype was dramatically aggravated and almost all HFs of mutant mice were defective (Fig. 2C, C′, and C″). The lower part of the HFs was widened, and often no clear hair bulb region was discernible. HSs had an irregular pigmentation pattern and were often misshapen or completely missing (Fig. C″, white arrowheads). Below SGs, normal ORS and IRS layers ended abruptly (white arrows) and unusual, large cells could be observed inside the HFs (black arrowheads). In adult skin, most of the nonpermanent regions of HFs were lost and no regrowth of anagen HFs was observed in the absence of Rac1. The upper part of the HFs, infundibula and SGs, were maintained throughout the whole life of the mutant mice (Fig. 2D and D′). Interestingly, SGs became enlarged with age (Fig. 2D′, arrowheads). Accumulations of melanin were often detected in the dermis and subcutis of adult mutant mice (Fig. 2D′, arrows). They were quite likely remnants of the lower part of the HFs. Mild fibrosis could be observed locally in the skin of adult mutant mice (data not shown). These findings indicated that Rac1 is required for maintenance of the nonpermanent part of the HFs.

Loss of HF-specific differentiation in the absence of Rac1. At 9 days, Rac1-deficient HF keratinocytes expressed characteristic marker proteins K6 (specific for CL; Fig. 3A and A′), K6irs2, K6irs4 (specific for IRS; Fig. 3B and B′ and 3C and C′), and Hb2 (specific for HS; Fig. 3D and D′). However, some mutant HFs already displayed a local loss of K6 (Fig. 3A′, arrowheads).

In 14-day-old mutant mice, expression of α6 integrin, which is normally present throughout the whole length of the HF at the basal side of the ORS cells adherent to the BM (Fig. 3E to H), ended abruptly shortly below the SGs (Fig. 3E′ to H′, arrowheads). The CL marker K6 was still present in the α6-positive regions (Fig. 3E′, black arrows) but absent or scattered below these regions (white arrow). IRS and HS markers were either entirely missing or present in nonconnected regions below the SGs (Fig. 3F′ to G′, white arrows).

K14, an ORS marker, was expressed normally only in the upper part of 14-day-old mutant HFs (Fig. 4A, A′, and A″). Interestingly, in the lower part of HFs, cells expressing K14, but not α6 integrin, were found, suggesting that fully differentiated ORS cells lost α6 integrin expression and thus polarization in the absence of Rac1 (Fig. 4A″, arrowheads). Also, a normal expression pattern of β-catenin, a cell-cell adhesion molecule, was lost in the lower region of the Rac1-deficient HFs (Fig. 4B, B′, and B″).

E-cadherin, another epithelial marker and adhesion protein, is expressed in all ORS cells of normal HF (Fig. 4C, C′, D, and D′). It was still present in HFs of 9-day-old mutant mice. However, the staining revealed an irregular shape of the ORS (Fig. 4C″, arrowheads) and distortions of hair bulbs (arrows). In 14-day-old mutant mice, E-cadherin was absent in the lower part of the HFs, below the α6 integrin expression region (Fig. 4D″, arrowheads).

Staining of DNA with DAPI showed the presence of nucleated cells in the lower part of mutant HFs, which did not express any epithelial or HF markers (Fig. 4B″, arrows; data not shown). IF detection of cells expressing vimentin, a mesenchymal intermediate filament protein (Fig. 5A, A′, and A″), revealed that the cells in the lower part of the mutant HFs were nonmesenchymal (Fig. 5A″, arrows), suggesting that they were indeed derived from epithelial keratinocytes of the HF.

Removal of the lower part of mutant HFs by macrophages. Distortions of HFs often trigger infiltration of phagocytic cells, for example, in β1 integrin-deficient mice (5). Therefore, we checked the back skin of control and mutant mice for the presence of macrophages and granulocytes.

A few evenly scattered macrophages, identified by Mac1 staining, were detected in the skin of 9- and 14-day-old control mice (Fig. 5B, B′, C, and C′, arrowheads). We did not observe an increased number of macrophages in the skin of 9-day-old mutant mice, although distorted HFs were already visible (Fig. 5B″, arrows). However, there was a massive infiltration of macrophages in the skin of 14-day-old Rac1-deficient mice (Fig. 5C″, arrows). The phagocytic cells were concentrated around the lower part of the mutant HFs, suggesting that macrophage-attracting signals were released by cells in this region. No granulocytes ($Gr\text{-}1^+$) were detected in the skin of 14-day-old control or mutant mice (data not shown). Phagocytes can be attracted by apoptotic cells (11). However, TUNEL staining did not reveal an increased amount of cells undergoing apoptosis in the lower part of mutant HFs, compared to control skin (Fig. 5D, D′, and D″).

No severe alterations of the epidermis in the absence of Rac1. In contrast to the HFs, the epidermis was almost not affected by the loss of Rac1. HE staining of back skin sections from 14-day-old mice did not reveal obvious alterations (Fig. 6A and A′). A BrdU incorporation assay of 14-day-old mouse skin indicated a similar proliferation rate of basal keratinocytes in normal and mutant epidermis (control, 10.3% $BrdU^+$ cells; KO, 11.4% $BrdU^+$ cells). No proliferation of Rac1-deficient suprabasal cells was detected (data not shown). In older mice,

FIG. 3. Loss of HF-specific differentiation in the absence of Rac1. IF staining of back skin sections from 9-day-old (A-D and A′-D′) and 14-day-old (E-H and E′-H′) control (ctrl) and mutant (KO) mice was carried out for the HF-specific keratins K6 (A and A′, E and E′), K6irs2 (B and B′, F and F′), K6irs4 (C and C′, G and G′), and Hb2 (D and D′, H and H′) (all in red). Counterstaining for α6 integrin (green) was used to outline BM and HFs. (A′-D′) At 9 days, expression of α6 integrin and distribution of keratins were mostly normal in Rac1-deficient HFs. However, K6 was already locally lost (A′; arrowheads). (E′-H′) In 14-day-old mutant skin, the expression of α6 integrin ended abruptly below SGs (arrowheads). K6 was still expressed in the regions along the α6-positive cells (E′; black arrows). In the lower part of HFs, normal expression of keratins was lost and only remnants could be detected in some cases (E′-G′; white arrows). Bars, 50 μm.

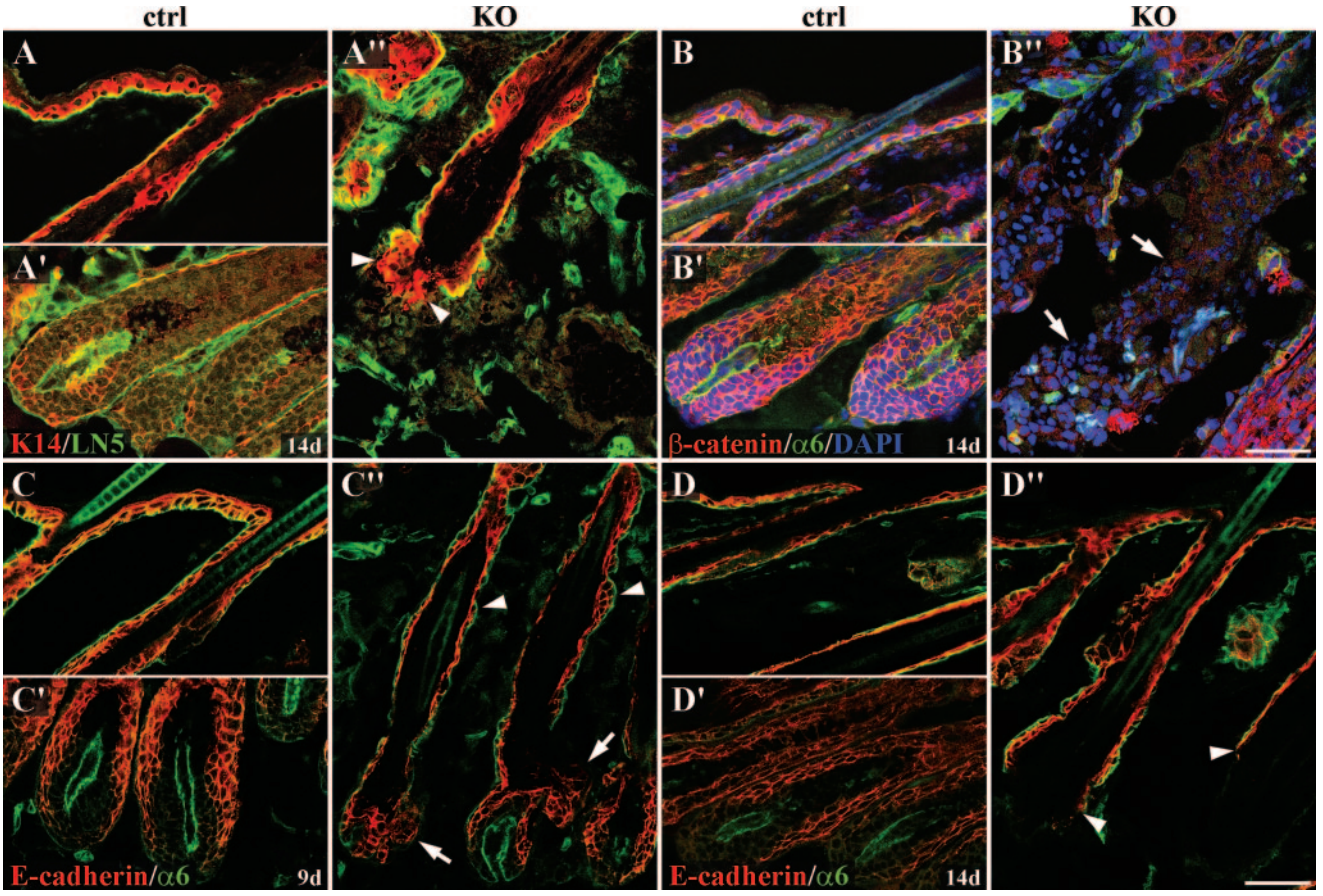

FIG. 4. Loss of ORS marker and adherens junction molecules in the lower part of Rac1 mutant HFs. IF staining of back skin sections from 9-day-old (C-C″) and 14-day-old (A-A″, B-B″, D-D″) control (ctrl) and mutant (KO) mice was carried out for the ORS marker K14 (A-A″), β-catenin (B-B″) and E-cadherin (C-C″, D-D″) (all in red). Counterstaining for α6 integrin (B-B″, C-C″, D-D″) or LN5 (A-A″) was used to outline BM and HFs (both in green). Nuclear DNA was visualized with DAPI (B-B″) (blue). (A″) K14 was absent in the lower part of mutant HFs. Some ORS cells had lost polarization (lack of α6 integrin expression) but still expressed K14 (arrowheads). (B″) Nucleated cells could still be observed in the lower part of mutant HFs, although β-catenin and α6 integrin expression was lost (arrows). (C″) In 9-day-old Rac1-deficient skin, E-cadherin staining showed changes in HF shape (arrowheads) and deformations of hair bulbs (arrows). (D″) Fourteen-day-old HFs of mutant mice lost E-cadherin expression below SGs, along with α6 integrin (arrowheads). Bars, 50 μm.

a slight thickening of the epidermis was observed in some regions, suggesting a local increase in proliferation (data not shown).

Expression of differentiation-specific keratins such as K14 (typical for basal keratinocytes; Fig. 6B and B′) and K10 (typical for suprabasal keratinocytes; Fig. 6C and C′), as well as loricrin (keratohyalin component typical for terminally differentiated keratinocytes; Fig. 6D and D′), was similar in 14-day-old control and mutant mice, indicating normal keratinocyte differentiation in the absence of Rac1. K6, which is aberrantly expressed in the epidermis under hyper- or hypoproliferative conditions, was not detected in the epidermis of Rac1 mutant or control mice (Fig. 6E and E′).

Studies with primary keratinocytes in vitro suggested defective cell-cell contacts in the absence of Rac1 (4). Surprisingly, IF staining for E-cadherin, β-catenin, α-catenin, and desmoplakin revealed a normal distribution of those junctional proteins in Rac1-null mouse epidermis (Fig. 6F to I and F′ to I′). Ultrastructural analysis confirmed the normal presence of adherens junctions (Fig. 6N and N′, white arrowheads) and desmosomes (Fig. 6M, M′, N, and N′, black arrows), although the intercellular distance between Rac1-deficient basal keratinocytes was sometimes increased compared to that in control mice.

Rac1 was found to be required for the assembly of laminin at the basal side and for the establishment of cell polarity in MDCK epithelial cysts grown in collagen (13). However, in 14-day-old Rac1 mutant mouse skin, deposition of the BM components LN5 and nidogen was normal and restricted to the dermal-epidermal junction (Fig. 6J to K and J′ to K′). Integrins α6 and β4 were expressed mainly at the basal side of the keratinocytes attached to BM, both in control and in mutant mice, further indicating that Rac1-null keratinocytes were polarized normally in the epidermis (Fig. 6L and L′). EM confirmed the deposition of a normal BM in the absence of Rac1 (Fig. 6M, M′, O, and O′, black arrowheads) and showed the presence of hemidesmosomes in both control and mutant mice (Fig. 6O and O′, white arrows). No blister formation was observed in Rac1-deficient skin, suggesting that adhesion of Rac1-null keratinocytes in vivo is normal or not altered suffi-

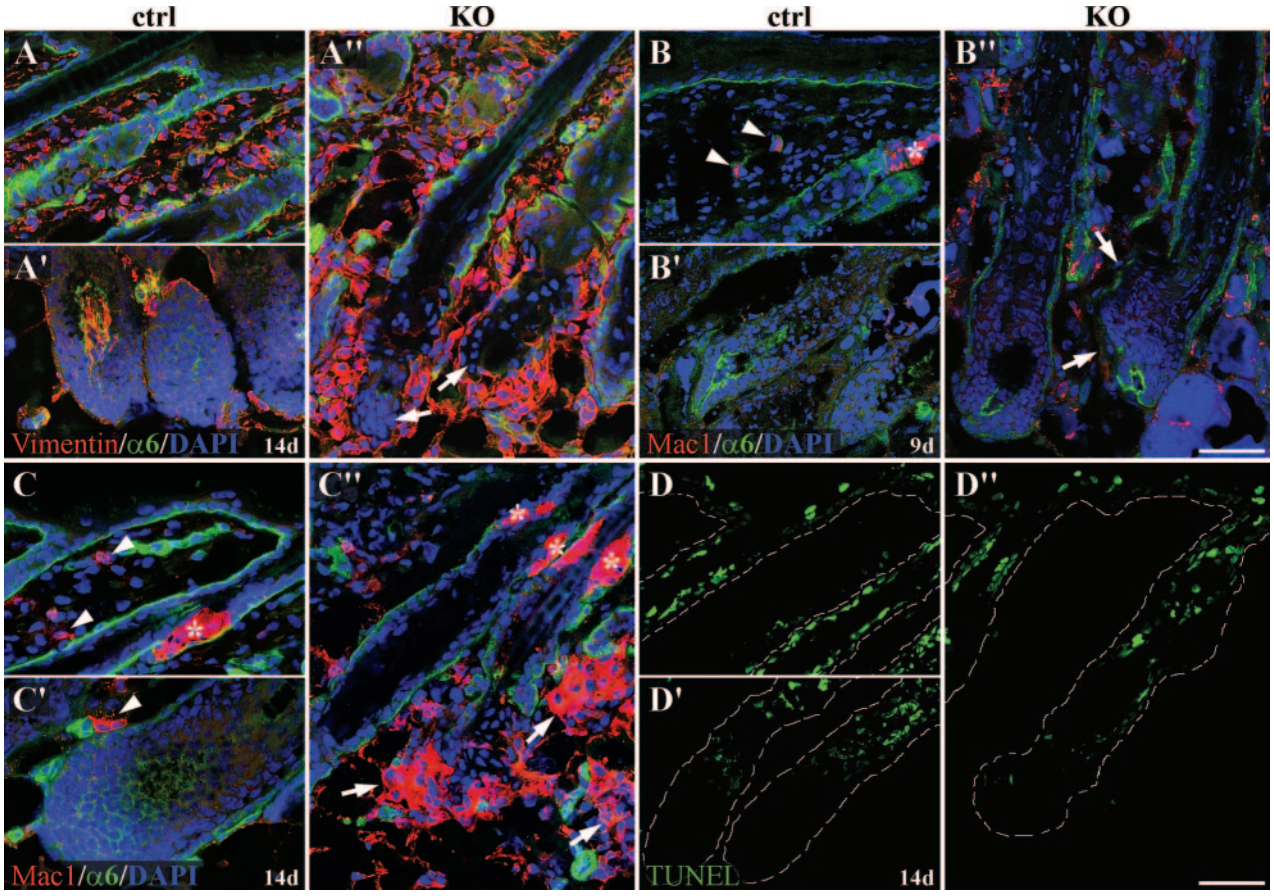

FIG. 5. Infiltration of macrophages in the skin of Rac1-deficient mice. IF staining of back skin sections from 9-day-old (B-B″) and 14-day-old (A-A″, C-C″) control (ctrl) and mutant (KO) mice was carried out for the mesenchymal marker vimentin (A and A″) and the macrophage marker Mac1 (B and B″, C and C″) (both in red). Counterstaining for α6 integrin was used to outline the BM and HFs (green). Nuclear DNA was visualized with DAPI (blue). (A″) Cells of the lower part of HFs, which had lost α6 integrin expression in the outermost layer, did not contain vimentin (arrows). (B and C) Only a few dispersed macrophages were found in the skin of 9-day-old and 14-day-old control mice (arrowheads). (B″) In 9-day-old mutant skin, no increased number of macrophages was detected, even around distorted hair bulbs (arrows). (C″) At 14 days, many $Mac1^+$ cells infiltrated the skin of mutant mice and were detected around the lower part of the HFs, which had lost α6 integrin expression in the outermost layer (arrows). Fluorescently labeled streptavidin, used as a secondary reagent, gave a nonspecific signal in SGs (B, C, C″; stars) and subcutaneous fat cells. Macrophages were also detected by anti-vimentin antibody (A″). (D, D′, and D″) No increase in $TUNEL^+$ cells was detected in the lower part of 14-day-old mutant HFs compared to control skin. Bars, 50 μm.

ciently to cause detachment of the epidermis from the underlying BM.

No significant changes in c-*Myc* expression or activation of NF-κB, JNK, p38, and Akt in Rac1-null epidermis. Recently, it was shown that induced loss of Rac1 in keratinocytes in vivo leads to increased expression of c-Myc, resulting in depletion of epidermal stem cells (1). However, we did not observe significant changes in the amount of c-Myc in epidermal lysates from Rac1 mutant mice at 3 days, 15 days, and 8 months of age compared to that in control samples (Fig. 7A).

To study more carefully the consequences of Rac1 deletion for different signaling pathways that were shown to be Rac1 dependent, we investigated the activation of NF-κB, JNK, p38, and Akt in the epidermis of Rac1 mutant mice. Activation of NF-κB was tested indirectly by measuring the amount of IκB-α which is degraded during activation of NF-κB. We could not detect changes in the activation levels of any of the proteins investigated in epidermal lysates from 3-day- and 8-month-old mice, indicating that Rac1 is not required for normal activation of these pathways in keratinocytes in vivo (Fig. 7B).

No obvious compensation for Rac1 absence by related Rho GTPases. To test whether loss of Rac1 leads to a compensatory upregulation of the expression of any closely related protein, we performed Western blot (Cdc42, RhoA, Rac2, and Rac3) or quantitative reverse transcription-PCR (RhoG) analysis. Cdc42 and RhoA protein levels were unchanged in 3-day- and 8-month-old Rac1 mutant mouse epidermis (Fig. 7C). While Rac2 was not detectable in epidermal lysates from 3-day-old control or mutant mice (data not shown), there were small amounts of the protein present in the epidermis of both control and mutant 8-month-old mice (Fig. 7C). We could not detect any Rac3 protein in lysates from the epidermis of 3-day-old and 8-month-old control or Rac1 mutant mice (data not shown and Fig. 7D, respectively). RhoG expression was determined in 3-month-old and 6-month-old mouse epidermis by quantitative reverse transcription-PCR with two independent

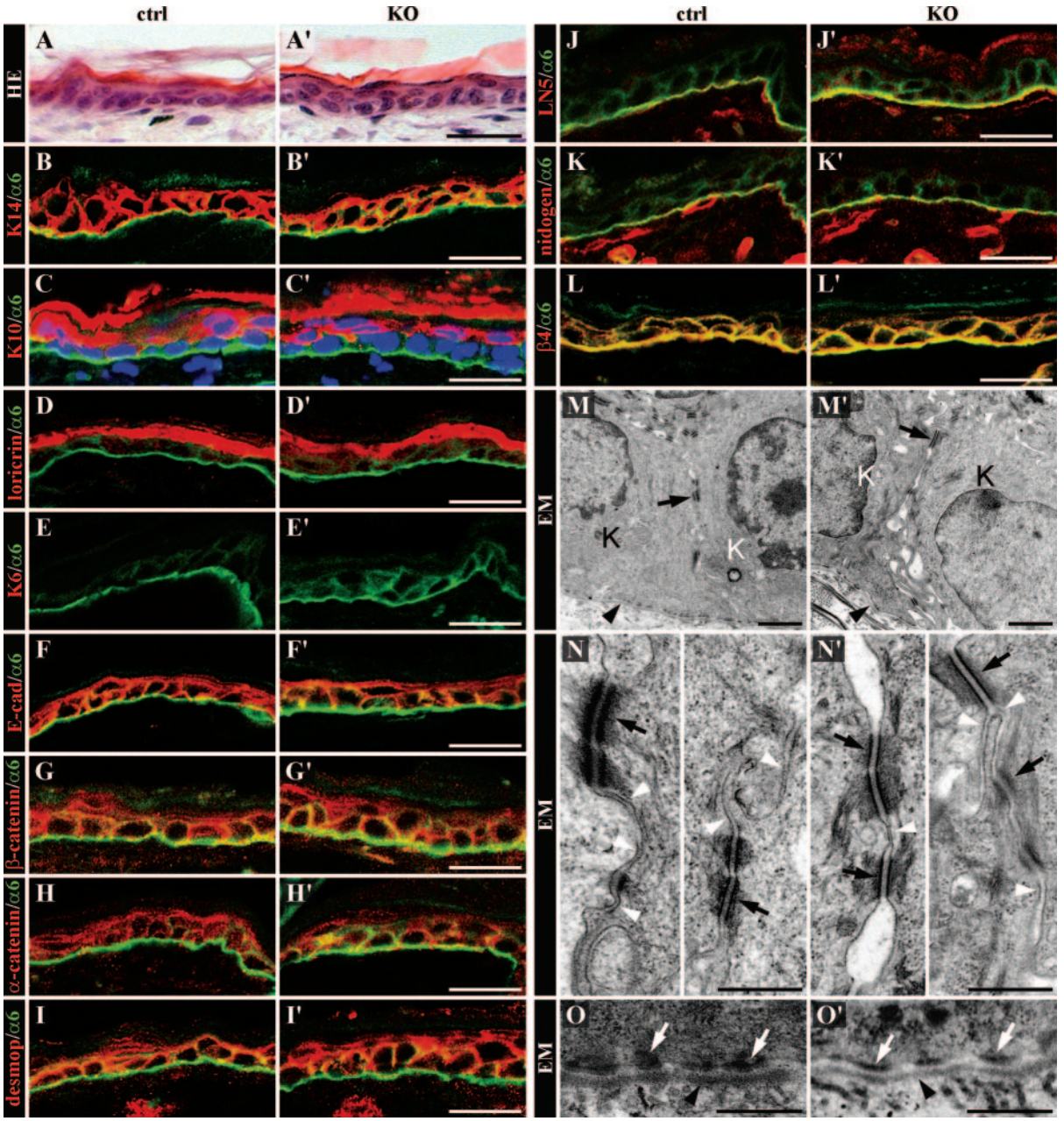

FIG. 6. Normal differentiation of the epidermis in the absence of Rac1. (A and A′) HE staining of back skin sections from 14-day-old control (ctrl) and mutant (KO) mice showed no changes in the morphology of the epidermis. (B to L and B′ to L′) IF staining of back skin sections from 14-day-old control and mutant mice was performed to investigate differentiation of the epidermis, the presence of cell-cell contacts, deposition of BM, and polarization of basal keratinocytes. No significant differences were observed between control and mutant mouse epidermis samples. Counterstaining for α6 integrin was used to demarcate the dermal-epidermal junction (green). Nuclear DNA was stained with DAPI (blue). The visualized proteins were (B and B′) the basal keratinocyte marker K14; (C and C′) the suprabasal keratinocyte marker K10; (D and D′) the terminal differentiation marker loricrin; (E and E′) the hyperproliferation marker K6; adherens junction molecules (F and F′) E-cadherin, (G and G′) β-catenin, and (H and H′) α-catenin; (I and I′) the desmosome component desmoplakin; BM molecules (J and J′) LN5 and (K and K′) nidogen; and (L and L′) β4 integrin (all in red). Bars, 25 μm (HE, IF). (M and M′) EM of back skin sections from 14-day-old mice showed the normal presence of desmosomes (black arrows) between basal keratinocytes (K) attached to BM (black arrowheads) in the absence of Rac1. Bar, 1 μm. (N and N′) Higher-magnification EM pictures of desmosomes (black arrows) and adherens junctions (white arrowheads) showed no defects in cell-cell contacts between Rac1-null keratinocytes. Bar, 0.5 μm. (O and O′) Higher-magnification EM pictures showed a normal structure of the BM (black arrowheads) and hemidesmosomes (white arrows) in control and mutant mice. Bar, 0.5 μm.

sets of primers. Neither of them showed a significant change in RhoG expression in the absence of Rac1 (data not shown and Fig. 7E).

Furthermore, we analyzed whether the amount of activated Cdc42, RhoA, or Rac2 is altered in the absence of Rac1. In neither 3-day-old nor in 8-month-old mouse epidermis was activation of Cdc42 or RhoA significantly affected by loss of Rac1 (Fig. 7C). We could not detect the active form of Rac2 in

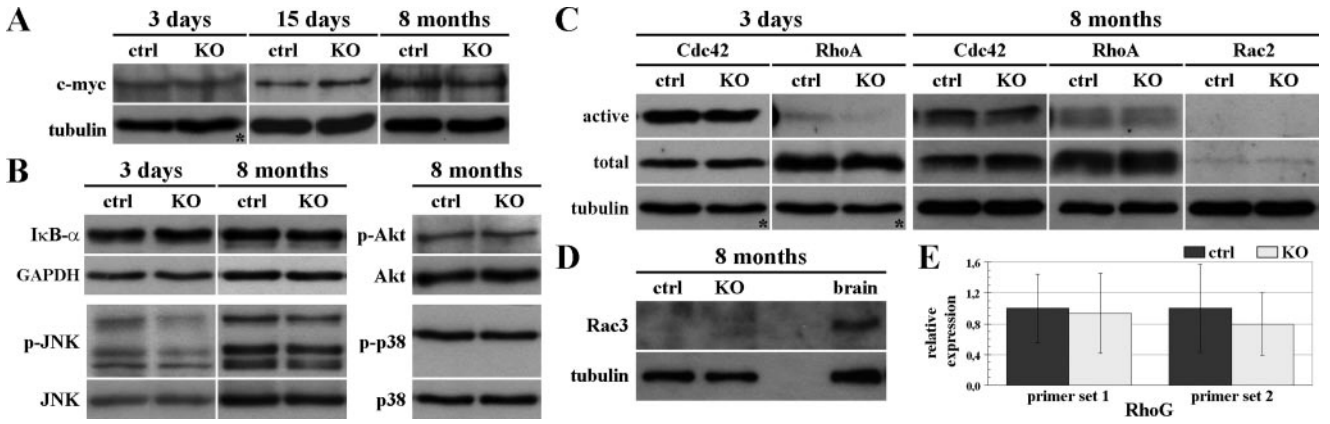

FIG. 7. Analysis of signaling pathway activation, protein expression, and activity of GTPases in Rac1-deficient epidermis. (A) Western blot analysis of c-Myc in epidermal lysates from 3-day-old, 15-day-old, and 8-month-old control (ctrl) and mutant (KO) mice showed no significant changes in expression of the protein in Rac1-deficient keratinocytes. Tubulin or GAPDH (*) content was used as a loading control. (B) Western blot analysis of signaling pathway activation in the epidermis of 3-day-old and 8-month-old control and mutant mice showed no significant changes in activation of NF-κB, JNK, Akt, or p38 in the absence of Rac1. Levels of IκB-α were checked as an indirect test of NF-κB activation. GAPDH content and total levels of JNK, Akt, and p38 were used as a loading control (p, phosphorylated forms). (C) Western blot analysis of GTPase activity performed with epidermal lysates from 3-day-old and 8-month-old control and mutant mice showed no significant differences in activation of Cdc42 or RhoA. The active form of Rac2 was not detected in lysates from 8-month-old mouse epidermis. Tubulin or GAPDH (*) content was used as a loading control. (D) No Rac3 protein was detected in epidermal lysates from 8-month-old control or mutant mice. Brain lysate was analyzed as a positive control, and tubulin content was used as a loading control. (E) Real-time PCR analysis of RhoG expression in 6-month-old mouse epidermis was performed with two different sets of primers. No significant changes in RhoG mRNA levels where detected in Rac1-null tissue in comparison to the control. GAPDH expression levels were used for standardization of samples.

epidermal lysates from 8-month-old control or mutant mice (Fig. 7C).

Although these data do not exclude compensatory changes in the expression or activation of other proteins in response to the absence of Rac1, they demonstrate that the proteins most likely capable of compensation are not involved.

Severe spreading defect of keratinocytes in vitro. We isolated primary keratinocytes from normal and Rac1-deficient mice in order to analyze them in cellular assays. However, it was not possible to sustain and expand mutant keratinocytes in vitro on Col/FN or on LN matrix, in contrast to normal keratinocytes (Fig. 8A and B). Nearly all Rac1-deficient cells died within a week, which might have been a secondary effect of the low number of initially (day 1) attached cells, as keratinocytes require quite a high cell density to survive and grow in vitro. Seeding mutant cells at a higher density did not rescue the culture, as the amount of attached cells after 24 h did not increase significantly.

To investigate the defect further, we performed adhesion assays under standard culture conditions. Surprisingly, the results revealed that within the first 2 h the adhesion of Rac1-null keratinocytes was only slightly reduced on Col/FN and similar on LN matrix compared to that of control cells (Fig. 8C).

In agreement with these data, primary Rac1-deficient keratinocytes showed normal cell surface expression of integrins α2, α6, β1, and β4 in a FACS analysis, whereas expression of integrins α1, α4, α5, αv, β2, β3, and β7 was not detectable in either type of cell (Fig. 8D and data not shown).

Next, we recorded, by time lapse video microscopy, the behavior of freshly isolated keratinocytes seeded on Col/FN-coated plastic. Adherent control cells were spreading normally and remained attached afterwards (see Movie S1 in the supplemental material). The majority of initially attached mutant keratinocytes, however, were not able to spread to the full extent (see Movie S2 in the supplemental material, first three arrows) or not at all (fourth arrow). Finally, most of the Rac-null adherent cells rounded up and detached, including some cells that were almost fully spread (last two arrows).

IF staining of cells attached to Col/FN showed that the majority of Rac1-deficient cells remained smaller than control keratinocytes, even after 3 days. Mutant cells formed paxillin-containing focal adhesions, but the actin cytoskeleton visualized with fluorescently labeled phalloidin seemed to be disorganized (Fig. 8E).

Quantitative analysis of the cell area confirmed that cell spreading is severely impaired in the absence of Rac1 (Fig. 8F). After 12 h, adherent control and mutant cells were comparable in size. However, during the next 24 h the size of Rac1-null keratinocytes remained unchanged, in contrast to that of normal keratinocytes, which continued to increase their cell area.

We did not observe a significant increase in cell death or terminal differentiation in adherent mutant cells within the first 24 h after seeding. Only 1.3% of the Rac1-null cells seeded on Col/FN and 2.2% of those seeded on LN matrix expressed large amounts of cleaved caspase 3, characteristic for apoptotic cells. These values were similar to those of the control, i.e., 0.4% and 2.2%, respectively. The amount of terminally differentiated cells, expressing loricrin, was about the same in mutant and control keratinocytes, i.e., 0.6% on the Col/FN-coated surface and 0.9% on the LN matrix. These results were in agreement with in vivo data.

Some cells isolated from mutant epidermis could adhere and spread like control cells (Fig. 8A and B, arrowheads). Most likely, these cells had escaped the deletion of the *rac1* gene and therefore still expressed the protein.

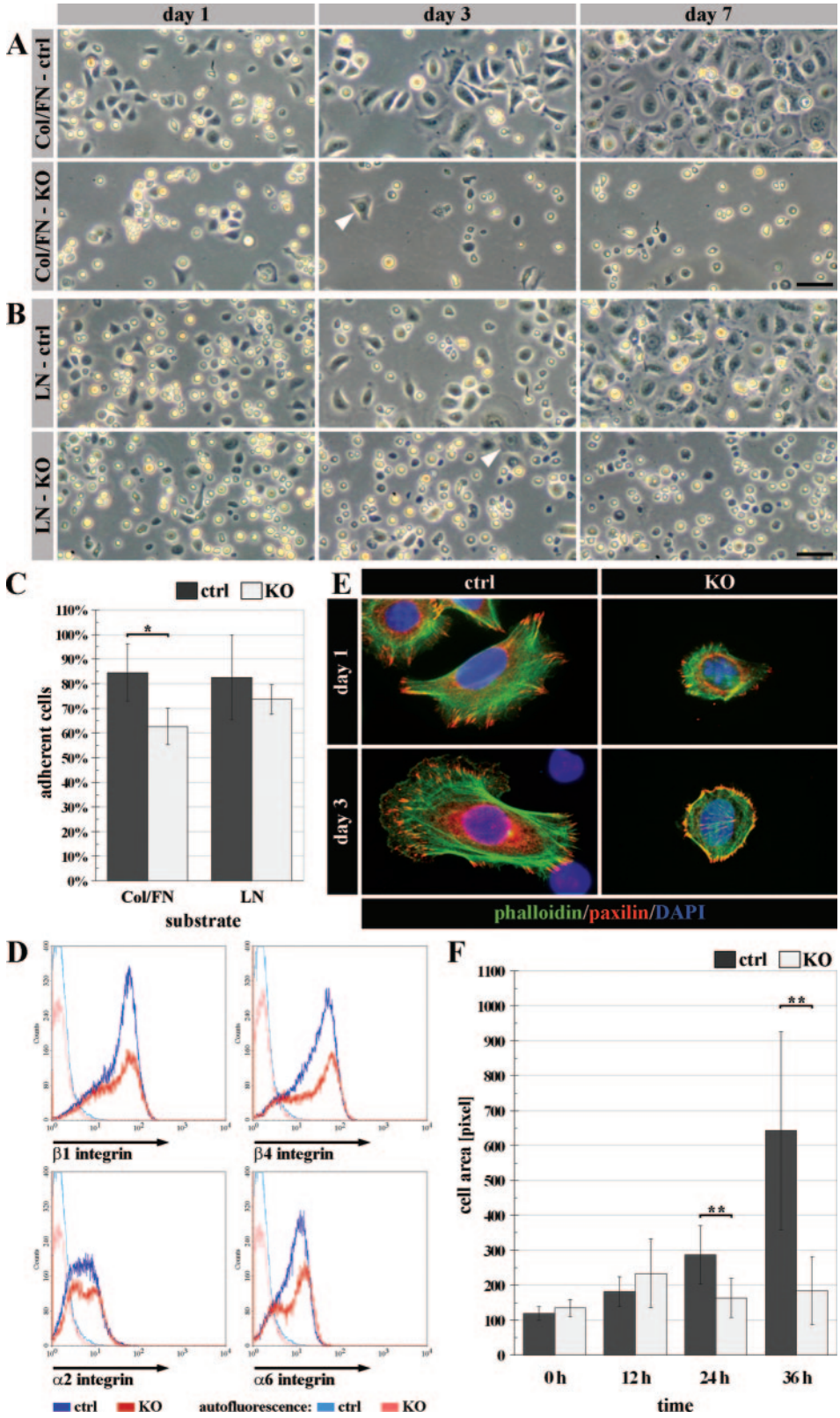

FIG. 8. Defective spreading of Rac1-null keratinocytes in vitro. Primary keratinocytes isolated from adult control (ctrl) and mutant (KO) mice seeded on (A) Col/FN-coated culture dishes or (B) LN matrix. On both substrates, a decreased number of attached Rac1-null cells was observed after 1 day, compared to control keratinocytes. Adherent mutant cells showed defective spreading and did not expand. Most of them died within a week. A few well-spread cells isolated from mutant mice (A and B, arrows) might have been cells that had escaped the deletion of the *rac1* gene. Bars, 50 μm. (C) Results of adhesion assays performed with freshly isolated control and mutant keratinocytes. Rac1-null cells

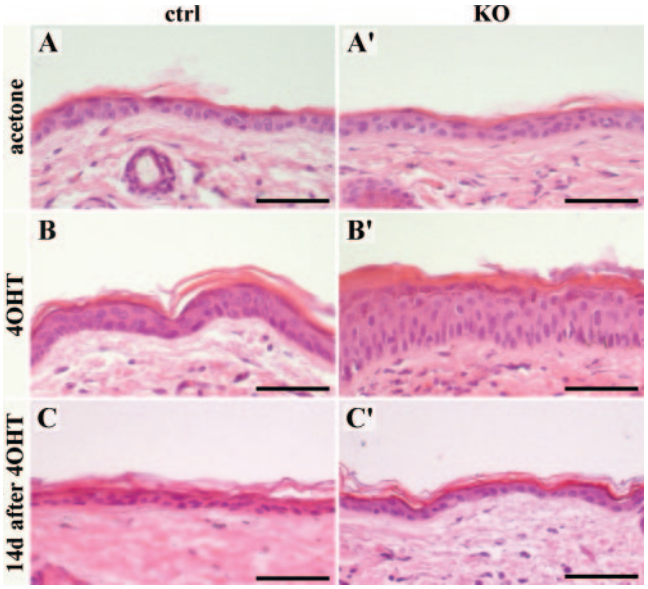

FIG. 9. Hyperthickening of Rac1-deficient epidermis caused by 4OHT application. HE staining of back skin sections from control (ctrl) and mutant (KO) mice treated with acetone alone (A and A′) or 4OHT-acetone (4OHT; B, B′, C, and C′) every 3 days for 15 days. The mice were sacrificed either 1 day (A, A′, B, and B′) or 2 weeks (C and C′) after the last application. 4OHT treatment resulted in transient hyperthickening of the Rac1 mutant epidermis. Bars, 50 μm.

Effect of 4OHT application on Rac1-deficient epidermis. It was recently reported that keratinocyte-specific deletion of the *rac1* gene induced in adult mice showed a severe phenotype with initial hyperthickening of the epidermis, followed by disorganization and decreased cellularity of the basal layer combined with increased cell size and finally partial or complete loss of epidermal keratinocytes (1). One of the explanations for the striking discrepancy between the two phenotypes could be the use of different methods leading to Rac1 removal. Repetitive application of 4OHT dissolved in acetone, used by Benitah and coworkers to induce the deletion, might have more severe consequences for Rac1-null epidermis than for normal skin.

To test that possibility, we applied acetone or 4OHT-acetone to a clipped area of back skin of control and Rac1-null mice every third day for 15 days. Acetone alone caused no obvious changes in control and mutant mouse epidermis (Fig. 9A and A′). Application of 4OHT-acetone, however, resulted in significant hyperthickening of the Rac1-deficient epidermis (Fig. 9B′). Mild alterations were also observed in control skin (Fig. 9B). Both phenotypes were transient, as 2 weeks after stopping the treatment, control and Rac1-null epidermis looked normal, indicating that 4OHT-acetone did not cause irreversible changes in keratinocyte stem cells (Fig. 9C and C′).

These data indicate that the treatment-related effects might have contributed to the phenotype of the mice with a 4OHT-induced deletion of the *rac1* gene (1). However, consequences of the treatment alone seem not to be sufficient to cause the phenotypic differences, suggesting the involvement of other factors such as compensatory mechanisms or the genetic background.

DISCUSSION

Following keratinocyte-restricted ablation of the *rac1* gene in mice, we observed a progressive loss of the lower part of the HF, while the SG, bulge region, and infundibulum were preserved. While a few days after birth HF morphogenesis was not obviously altered in the absence of Rac1, by day 14 the majority of HFs lost their normal appearance. Development of constrictions and loss of HF integrity indicate changes in cell-cell contacts between keratinocytes in the lower part of mutant HFs. A focal absence in 9-day-old HFs and the total loss of characteristic HF proteins in the lower region of 14-day-old HFs suggest involvement of Rac1 in the regulation of gene expression. As we did not detect an increased apoptosis in mutant HFs, it is unlikely that the loss of HFs is related to premature induction of catagen, when the nonpermanent part of the HF is removed by apoptotic involution as part of the normal hair cycle. Apparently, Rac1 contributes to the maintenance of a differentiated state of HF keratinocytes in the nonpermanent part of the follicle.

During IRS formation, Huxley "Flügelzellen" penetrate through the lower, less differentiated part of the Henle layer to come in contact with CL keratinocytes in a process apparently dependent on the formation of lamellipodia (9). Loss of Rac1 might impair this migration, thus contributing to HF malformation during morphogenesis.

The changes in the HFs led to an infiltration of macrophages, which subsequently removed the nonpermanent part of the HFs. No invasion of granulocytes and only a very mild fibrosis were observed, in contrast to the phenotype of mice lacking β1 integrin in keratinocytes, where the infiltration of macrophages and granulocytes is caused by severe deformation of the HFs and results in complete removal of the HFs and severe fibrosis (5).

The absence of anagen HFs in Rac1 mutant mice after HF morphogenesis might be caused by a defect in HF-specific progenitor cells located in the hair bulge region. Alternatively, it could be a result of their impaired activation, as signaling

showed slightly impaired attachment to Col/FN (*, $P < 0.005$) and no significant reduction in adhesion to LN matrix. (D) The cell surface expression of integrins β1, β4, α2, and α6 was investigated by FACS analysis of primary keratinocytes from adult control (dark blue) and mutant (red) mice. The presence of integrin on the cell surface of basal (high peak) and suprabasal keratinocytes (lower peak or shoulder) was normal in Rac1-null keratinocytes. The relative amount of mutant suprabasal cells was slightly higher. (E) Primary control and mutant keratinocytes were stained for F-actin (phalloidin; green), paxillin (red), and nuclear DNA (DAPI; blue) 1 and 3 days after isolation. Results indicated impaired actin cytoskeleton organization in Rac1-null keratinocytes but showed formation of focal adhesions. Cells were seeded on Col/FN-coated glass. (F) Spreading of primary keratinocytes after seeding on Col/FN-coated plastic. Cell size was analyzed by measuring the pixel area of 30 to 40 randomly chosen control and mutant cells at the time points indicated. Initially, there were no significant differences between the cells. However, after 12 h, Rac1-null cells stopped spreading while control cells continued to increase in size (**, $P < 0.0001$).

between the mesenchyme and bulge stem cells, required for anagen induction, might be affected in the absence of Rac1.

In contrast to the severe defects in the lower part of the HFs, the upper part of the HFs and the epidermis were only mildly affected. Also, the SGs, which are derived from bulge stem cells, were maintained in the absence of Rac1. Only an increased intercellular distance between some of the basal keratinocytes in the epidermis, as revealed by ultrastructural analysis, indicated that the function of Rac1 is not completely redundant in the epidermis.

We did not see changes in the activation of potentially Rac1-dependent signaling pathways such as JNK, p38, Akt, and NF-κB in mutant epidermis. It is possible that deletion of the *rac1* gene in keratinocytes is compensated for by increased expression or activation of other Rho GTPases with redundant functions (8). However, when we investigated mRNA expression of RhoG or protein expression and activity of Cdc42, Rac2, Rac3, and RhoA in the epidermis of Rac1 mutant mice, we did not detect any significant changes. Apparently, the most closely related members of the Rac1 family are not involved in a compensatory response to the loss of Rac1.

Contrary to the subtle phenotype in the epidermis, primary Rac1-null keratinocytes displayed severely impaired spreading and were prone to detachment when seeded on Col/FN or LN matrix in vitro. As in vivo, however, we did not detect increased apoptosis or terminal differentiation of Rac1-deficient keratinocytes. The spreading defect observed in vitro might correlate with the very subtle changes in cell-cell distance observed by EM in mutant epidermis.

Recently, it has been shown that induced loss of Rac1 in keratinocytes of adult mice leads to severe deterioration of the epidermis due to depletion of epidermal stem cells (1). In our Rac1-deficient mice, where the gene deletion was activated endogenously during embryogenesis, the epidermis was maintained even in 24-month-old mice, although hardly any Rac1 protein was detectable in epidermal lysates. These data clearly show that the presence of Rac1 is not indispensable for stem cell maintenance in the epidermis. It might be, however, that deletion of the *rac1* gene during embryonic development allows for a compensatory response that cannot be initiated in adult tissue. Another likely reason for the contrasting results is the different genetic background of the mice used in our study. In epidermal growth factor receptor-deficient mice, for example, the phenotype varies from placental defects to postnatal defects in the skin, lung, and brain, depending on the strain of analyzed mice (19). Finally, our data suggest that effects related to the 4OHT-acetone treatment might have contributed to the differences between two Rac1-deficient mutant mice.

ACKNOWLEDGMENTS

We thank Michael Bösl for blastocyst injection, Jose Jorcano for K5 Cre mice, David Ermert for help during histological analysis, Ursula Kuhn and Elke Heyder for expert technical assistance, Fiona Watt for sharing unpublished observations, Arnoud Sonnenberg for advice and LN5-producing cells, Kyle Legate for reading the manuscript, Carsten Grashoff for help with manuscript revision, and Reinhard Fässler for generous support and helpful discussions.

This work was supported by the German Research Council (DFG) and the Max Planck Society.

REFERENCES

1. **Benitah, S. A., M. Frye, M. Glogauer, and F. M. Watt.** 2005. Stem cell depletion through epidermal deletion of Rac1. Science **309:**933–935.
2. **Bolis, A., S. Corbetta, A. Cioce, and I. de Curtis.** 2003. Differential distribution of Rac1 and Rac3 GTPases in the developing mouse brain: implications for a role of Rac3 in Purkinje cell differentiation. Eur. J. Neurosci. **18:**2417–2424.
3. **Braga, V. M. M., M. Betson, X. Li, and N. Lamarche-Vane.** 2000. Activation of the small GTPase Rac is sufficient to disrupt cadherin-dependent cell-cell adhesion in normal human keratinocytes. Mol. Biol. Cell **11:**3703–3721.
4. **Braga, V. M. M., L. M. Machesky, A. Hall, and N. A. Hotchin.** 1997. The small GTPases Rho and Rac are required for the establishment of cadherin-dependent cell-cell contacts. J. Cell Biol. **137:**1421–1431.
5. **Brakebusch, C., R. Grose, F. Quondamatteo, A. Ramirez, J. L. Jorcano, A. Pirro, M. Svensson, R. Herken, T. Sasaki, R. Timpl, S. Werner, and R. Fassler.** 2000. Skin and hair follicle integrity is crucially dependent on β1 integrin expression on keratinocytes. EMBO J. **19:**3990–4003.
6. **Caldelari, R., M. M. Suter, D. Baumann, A. de Bruin, and E. Muller.** 2000. Long-term culture of murine epidermal keratinocytes. J. Investig. Dermatol. **114:**1064–1065.
7. **Delwel, G. O., F. Hogervorst, I. Kuikman, M. Paulsson, R. Timpl, and A. Sonnenberg.** 1993. Expression and function of the cytoplasmic variants of the integrin alpha 6 subunit in transfected K562 cells. Activation-dependent adhesion and interaction with isoforms of laminin. J. Biol. Chem. **268:**25865–25875.
8. **Jaffe, A. B., and A. Hall.** 2005. Rho GTPases: biochemistry and biology. Annu. Rev. Cell Dev. Biol. **21:**247–269.
9. **Langbein, L., M. A. Rogers, S. Praetzel, H. Winter, and J. Schweizer.** 2003. K6irs1, K6irs2, K6irs3, and K6irs4 represent the inner-root-sheath-specific type II epithelial keratins of the human hair follicle. J. Investig. Dermatol. **120:**512–522.
10. **Langbein, L., and J. Schweizer.** 2005. Keratins of the human hair follicle. Int. Rev. Cytol. **243:**1–78.
11. **Lauber, K., S. G. Blumenthal, M. Waibel, and S. Wesselborg.** 2004. Clearance of apoptotic cells: getting rid of the corpses. Mol. Cell **14:**277–287.
12. **Mertens, A. E. E., T. P. Rygiel, C. Olivo, R. van der Kammen, and J. G. Collard.** 2005. The Rac activator Tiam1 controls tight junction biogenesis in keratinocytes through binding to and activation of the Par polarity complex. J. Cell Biol. **170:**1029–1037.
13. **O'Brien, L. E., T.-S. Jou, A. L. Pollack, Q. Zhang, S. H. Hansen, P. Yurchenco, and K. E. Mostov.** 2001. Rac1 orientates epithelial apical polarity through effects on basolateral laminin assembly. Nat. Cell Biol. **3:**831–838.
14. **Osoegawa, K., M. Tateno, P. Y. Woon, E. Frengen, A. G. Mammoser, J. J. Catanese, Y. Hayashizaki, and P. J. de Jong.** 2000. Bacterial artificial chromosome libraries for mouse sequencing and functional analysis. Genome Res. **10:**116–128.
15. **Price, L. S., M. Langeslag, J. P. ten Klooster, P. L. Hordijk, K. Jalink, and J. G. Collard.** 2003. Calcium signaling regulates translocation and activation of Rac. J. Biol. Chem. **278:**39413–39421.
16. **Ramirez, A., A. Page, A. Gandarillas, J. Zanet, S. Pibre, M. Vidal, L. Tusell, A. Genesca, D. A. Whitaker, D. W. Melton, and J. L. Jorcano.** 2004. A keratin K5Cre transgenic line appropriate for tissue-specific or generalized cre-mediated recombination. Genesis **39:**52–57.
17. **Romero, M. R., J. M. Carroll, and F. M. Watt.** 1999. Analysis of cultured keratinocytes from a transgenic mouse model of psoriasis: effects of suprabasal integrin expression on keratinocyte adhesion, proliferation and terminal differentiation. Exp. Dermatol. **8:**53–67.
18. **Schmidt-Ullrich, R., and R. Paus.** 2005. Molecular principles of hair follicle induction and morphogenesis. Bioessays **27:**247–261.
19. **Sibilia, M., J. P. Steinbach, L. Stingl, A. Aguzzi, and E. F. Wagner.** 1998. A strain-independent postnatal neurodegeneration in mice lacking the EGF receptor. EMBO J. **17:**719–731.
20. **Sonnenberg, A., A. A. de Melker, A. M. Martinez de Velasco, H. Janssen, J. Calafat, and C. M. Niessen.** 1993. Formation of hemidesmosomes in cells of a transformed murine mammary tumor cell line and mechanisms involved in adherence of these cells to laminin and kalinin. J. Cell Sci. **106:**1083–1102.
21. **Wennerberg, K., and C. J. Der.** 2004. Rho-family GTPases: it's not only Rac and Rho (and I like it). J. Cell Sci. **117:**1301–1312.